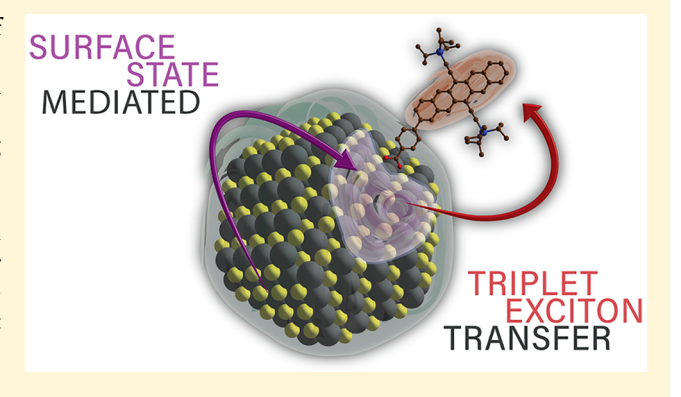


# Surface States Mediate Triplet Energy Transfer in Nanocrystal—Acene **Composite Systems**

Jon A. Bender,  $^{\perp,\dagger_{0}}$  Emily K. Raulerson,  $^{\perp,\dagger}$  Xin Li,  $^{\ddagger}$  Tamar Goldzak,  $^{\$}$  Pan Xia,  $^{\parallel_{0}}$  Troy Van Voorhis,  $^{\$}$  Ming Lee Tang,  $^{\ddagger,\parallel_{0}}$  and Sean T. Roberts\*,  $^{\dagger_{0}}$ 

Supporting Information

ABSTRACT: Hybrid organic:inorganic materials composed of semiconductor nanocrystals functionalized with acene ligands have recently emerged as a promising platform for photon upconversion. Infrared light absorbed by a nanocrystal excites charge carriers that can pass to surface-bound acenes, forming triplet excitons capable of fusing to produce visible radiation. To fully realize this scheme, energy transfer between nanocrystals and acenes must occur with high efficiency, yet the mechanism of this process remains poorly understood. To improve our knowledge of the fundamental steps involved in nanoparticle:acene energy transfer, we used ultrafast transient absorption to investigate excited electronic dynamics of PbS nanocrystals chemically functionalized with 6,13-bis-



(triisopropylsilylethynyl)pentacene (TIPS-pentacene) ligands. We find photoexcitation of PbS does not lead to direct triplet energy transfer to surface-bound TIPS-pentacene molecules but rather to the formation of an intermediate state within 40 ps. This intermediate persists for ~100 ns before evolving to produce TIPS-pentacene triplet excitons. Analysis of transient absorption lineshapes suggests this intermediate corresponds to charge carriers localized at the PbS nanocrystal surface. This hypothesis is supported by constrained DFT calculations that find a large number of spin-triplet states at PbS NC surfaces. Though some of these states can facilitate triplet transfer, others serve as traps that hinder it. Our results highlight that nanocrystal surfaces play an active role in mediating energy transfer to bound acene ligands and must be considered when optimizing composite NC-based materials for photon upconversion, photocatalysis, and other optoelectronic applications.

# INTRODUCTION

Hybrid materials composed of inorganic semiconductor nanocrystals (NCs) and organic acene molecules have emerged as a promising platform for photonic devices that repartition the quanta of incoherent light. High energy photons absorbed by members of the acene family can initiate singlet fission, an energy down-conversion process wherein an absorbed photon leads to the creation of two spin-triplet excitons, each with roughly half of the photon's energy. This energy can be subsequently passed to semiconductor NCs<sup>3,4</sup> and re-emitted as two infrared photons, used to drive catalytic conversions, 5 or power photovoltaic circuits. 6-8 Similarly, excitons in semiconductor NCs created by infrared light absorption can be transferred to surface-bound acene molecules to produce triplet excitons. 9-12 Once triplet excitons are generated in sufficient numbers, they may combine to yield high-energy spin-singlet excitons that can emit visible light. By altering either acene chemical structure or NC size and shape, the relative energy

levels of these materials can be tuned to direct energy flow for either photon up-conversion or down-conversion.

Ensuring efficient energy transfer across the acene:NC interface is critical to the success of photonic devices using these materials. However, the mechanism of this form of energy transfer remains poorly understood. The acene family's spinsinglet ground state and low intrinsic spin-orbit coupling make radiative transitions to and from spin-triplet excited states spinforbidden. 13,14 Consequently, it is broadly postulated that triplet energy transfer between NCs and acene molecules must unfold via a Dexter-type mechanism wherein electron exchange plays an integral role. 3,4,10,15,16 Under this scenario, the distance between acenes and the NC surface as well as the orientation of acenes with respect to the NC surface are critical to control as wave function overlap between these materials is required for energy transfer. 17 Despite this challenge, energy transfer time

Received: February 16, 2018 Published: May 30, 2018

<sup>&</sup>lt;sup>†</sup>Department of Chemistry, The University of Texas at Austin, Austin, Texas 78712, United States

<sup>\*</sup>Department of Chemistry, University of California Riverside, Riverside, California 92521, United States

Department of Chemistry, Massachusetts Institute of Technology, Cambridge, Massachusetts 02139, United States

Materials Science & Engineering Program, University of California Riverside, Riverside, California 92521, United States

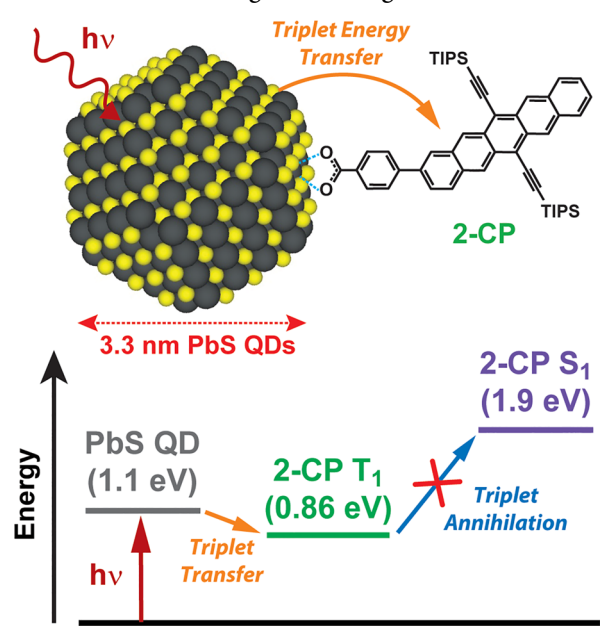
scales as fast as 1 ps have been reported for triplet energy transfer between pentacene triplet excitons and PbSe NCs terminated with benzenedithiol ligands.<sup>3</sup> In stark contrast, rates for triplet energy transfer from NCs to acene molecules are much more modest, falling in the range of hundreds of picoseconds to hundreds of nanoseconds.<sup>10,11,15,18–22</sup> Slow rates of transfer are even seen when acenes are directly bound to nanoparticle surfaces via short covalent tethers.<sup>10,19,20,23</sup> The origin of the apparent disparity between rapid triplet energy transfer from acenes to NCs and the relatively slow reverse process is not immediately clear.

One possible explanation for the slow rate of energy transfer from NCs to acenes is an increase in the local dielectric constant felt by acene molecules in close proximity to NC surfaces provides additional Coulombic screening that slows triplet energy transfer. 15 Though this effect may be significant in solid films, where NCs are in close proximity and the effective dielectric of the medium approaches that of the bulk semiconductor, it does not account for slow triplet energy transfer rates seen for solution-phase NCs functionalized with covalently bound acene ligands as they experience an effective dielectric constant closer to that of the surrounding solvent. Additionally, changes in the local dielectric constant should similarly affect triplet energy transfer from acenes to semiconductor NCs, but relatively rapid energy transfer rates for this process have been observed in solid films.<sup>3,4</sup> Alternatively, triplet energy transfer from NCs to surface-bound acenes may not proceed through a concerted Dexter-like mechanism but rather a sequential process involving multiple steps. Recent work examining triplet energy transfer between PbS NCs and TIPS-pentacene molecules covalently anchored to their surfaces identified two sequential kinetic events resulting in TIPS-pentacene triplet exciton production.<sup>20</sup> These two processes were assigned to successive charge transfer events, the first being hole transfer on a sub-100 ps time scale followed by electron transfer over ~6 ns. The slow rate of electron transfer, relative to hole transfer, was attributed to energetic mismatch of the PbS NCs' conduction band edge and the triplet exciton molecular orbitals of TIPS-pentacene. However, the absence of a photobleach associated with the TIPSpentacene cation on intermediate time scales leads us to question this interpretation.

Rather, the slow rate of energy transfer from NCs to acenes may point to the involvement of NC midgap states that trap charge carriers. Improper passivation of NC surfaces is well-known to lead to the creation of localized surface states. 24–29 Formation of these states could impact triplet energy transfer by both altering the energy of photoexcited carriers and wave function overlap with surface-bound acene molecules. Indeed, work that examined CdSe NCs functionalized with anthracene derivatives found the yield of upconverted light depended critically on the photoluminescence quantum yield of the NCs prior to anthracene functionalization, 30 suggesting defect state formation competes with triplet energy transfer to anthracene.

In an effort to elucidate the mechanistic pathways that facilitate triplet energy transfer from semiconductor NCs to acene molecules, we have used femtosecond transient absorption to examine the excited state dynamics of PbS NCs functionalized with 4-(6,13-bis(2-(triisopropylsilyl)-ethynyl)pentacen-2-yl)benzoic acid (2-CP). A Jablonski diagram illustrating the relative energy levels of excitonic states and open energy transfer pathways associated with this system is provided in Scheme 1. We elected to study 2-CP

Scheme 1. (Top) Cartoon Illustrating 2-CP Structure and Expected Attachment Geometry to a PbS NC (in addition to 2-CP, PbS surfaces contain oleate ligands; (Bottom) Jablonski Plot Illustrating State Energies for PbS and 2-CP



functionalized NCs because photon upconversion via triplet exciton annihilation should be suppressed due to 2-CP's sufficiently low triplet exciton energy, thereby allowing us to more easily identify steps involved in triplet exciton formation. We find photoexcitation of PbS indeed results in 2-CP triplet exciton formation on a ~100 ns time scale, in accordance with triplet exciton formation rates reported for other NC:acene systems. 10,11,15,18-21 However, these triplet excitations are not created directly from PbS bandedge states associated with the NC bulk but are instead formed via a kinetic intermediate. The evolution of spectral changes seen within the first few picoseconds following PbS photoexcitation provide strong evidence this intermediate corresponds to an excitation localized at the PbS NC surface. We find these states are not formed by PbS NCs prior to 2-CP ligand exchange, leading us to conclude the exchange process used to attach 2-CP to PbS NCs produces surface sites that quickly localize excitations. Interestingly, saturating these states with pump fluences capable of producing multiple excitations per NC significantly speeds triplet energy transfer, suggesting their net effect is to trap excitations and slow triplet formation. However, quantum chemical calculations suggest a subtler picture as they reveal some of these states weakly interact with surface-bound 2-CP molecules and serve as exciton traps whereas others are coupled to 2-CP molecules and facilitate NC-to-ligand energy transfer. Our results indicate NC surface states play an active role in modifying triplet energy transfer rates to surface-bound ligands and must be considered when designing composite NC-based materials for photon upconversion, photocatalysis, and other optoelectronic applications.

# EXPERIMENTAL AND COMPUTATIONAL METHODS

**Material Synthesis.** 2-CP was prepared by synthesizing a brominated TIPS-pentacene derivative according to the methods of Sanders et al.<sup>31</sup> that was then further modified to add a benzoic acid linker. Detailed synthesis procedures are included in the Supporting

Information. PbS NCs were produced following our previously published methods.<sup>32</sup>

**2-CP Ligand Exchange.** 2-CP was dissolved in 200 μL of tetrahydrofuran. To this solution was added a toluene solution containing PbS NCs, to bring the total volume of the combined solution to 1.25 mL. Prior to mixing, the concentration of PbS NCs in the initial toluene solution was adjusted such that the NC concentration in the combined PbS:2-CP solution is 10 μM. The amount of 2-CP in the combined solution was selected to yield either a 50 or 500 molar excess relative to the number of NCs in solution. This combined solution was stirred for 40 min to facilitate ligand exchange. To isolate 2-CP functionalized NCs, 4 mL of an antisolvent, acetone, was added to precipitate the NCs. The solution was centrifuged, the resulting supernatant was discarded, and the pellet containing 2-CP functionalized NCs redispersed in toluene. As 2-CP molecules not adhered to PbS largely remain in the supernatant, this process also serves to remove unbound 2-CP molecules from solution.

Steady-State Characterization of NC Solutions. Absorption spectra of NCs suspended in toluene were measured using a Shimadzu UV-2600 absorption spectrometer with an integrating sphere attachment. The ratio of PbS NCs to 2-CP molecules in solution was determined by comparing the amplitude of absorption features for each species to extinction values we determined for 2-CP ( $\varepsilon=19\,200\,M^{-1}\,$  cm $^{-1}$  at  $\lambda_{\rm max}=651\,$  nm) and values reported for PbS ( $\varepsilon=61\,500\,M^{-1}\,$  cm $^{-1}$  at  $\lambda_{\rm max}=1005\,$  nm). As the continuum absorption band for PbS overlaps with absorption features from 2-CP, the absorption spectrum of oleate-capped PbS NCs was subtracted from the spectrum of the 2-CP:PbS solution prior to calculating the 2-CP concentration.

Transient Absorption Measurements of NC Solutions. TA measurements were performed using the output of a Ti:sapphire amplifier with a center wavelength of 804 nm (Coherent Duo Legend Elite, 3 kHz, 4.5 mJ). For femtosecond-resolution measurements, a portion of the amplifier output was used as the excitation pulse whereas white light supercontinuum probe pulses were produced by focusing  $0.5-1 \mu J$  of the amplifier's output into either a 3 mm thick ccut sapphire plate or a 6 mm thick undoped Yttrium Aluminum Garnet (YAG) crystal. A mechanical delay stage controlled the pumpprobe time delay (Newport ILS300LM) and changes in the probe transmission were detected using two different detectors, a silicon CCD camera (Princeton Instruments PyLoN 100-BR) for visible wavelengths and a 512-pixel InGaAs linear imaging sensor (Hamamatsu G11620-512DA) for infrared wavelengths, following dispersal of the probe by a 500 mm Czerny-Turner spectrometer (Acton Instruments Spectra Pro 2556). To measure TA spectra over nanosecond-to-millisecond time delays, the excitation source was replaced with the 1064 nm output of an independently triggered Qswitched Nd:YAG laser (Alphalas Pulselas-A, <1 ns, 8.7 µI). A digital delay generator (Stanford Research Systems DG535) synchronized the pump laser's operation with the Ti:sapphire amplifier.

NC samples for TA measurements were suspended in toluene and housed in a 1 mm path length cuvette. Samples were continuously stirred throughout data collection and were diluted such that their optical densities were 0.1 or less at the peak of the PbS X1 absorption band. All TA spectra reported in the main paper were measured with perpendicularly polarized pump and probe fields to minimize contributions to TA spectra from nonresonant backgrounds arising from the solvent and sample cuvette. Though in principle this allows contributions to TA spectra that stem from reorientation of the transition moment of the PbS state produced by the excitation pulse, prior work has shown the TA anisotropy of PbS NCs is negligible.<sup>34</sup> Data presented in Figures 1 and 6 were recorded for a 2-CP:PbS sample containing 25.7 2-CP molecules per NC, whereas data in Figures 2, 3, and 5 were measured for a sample with a slightly higher 2-CP:NC ratio of 46.2:1. No quantitative differences were observed in the transient behavior of these samples and hence we do not postulate their difference in 2-CP concentration has a substantive impact on the conclusions we draw regarding the mechanism of triplet energy transfer from PbS to 2-CP.

**Computational Methodology.** Constrained density functional theory<sup>35</sup> was used to locate different spin-triplet states of a PbS NC

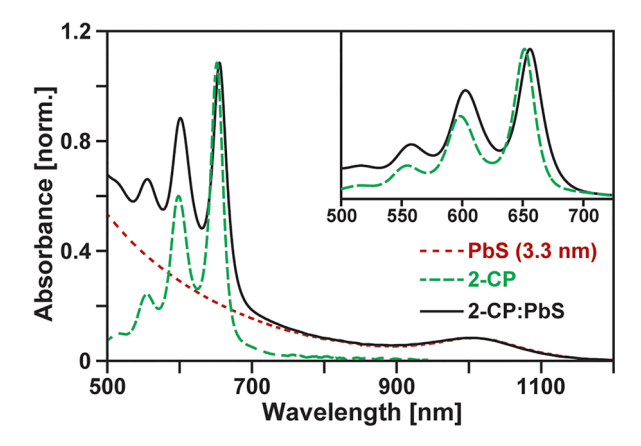
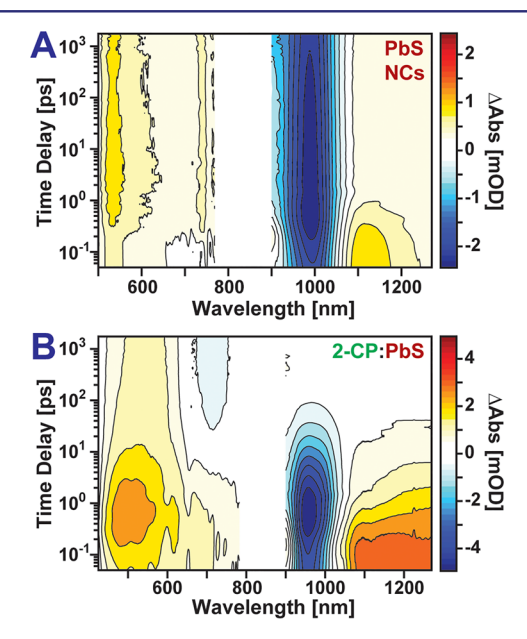


Figure 1. Absorption spectra of 2-CP (green, long dash), oleate-functionalized PbS NCs (red, short dash), and 2-CP:PbS (black). (Inset) Zoomed-in view of the 2-CP absorption region following subtraction of PbS contributions to the spectra. All spectra were measured in toluene. Features arising from the solvent have been subtracted.



**Figure 2.** TA spectra of (A) oleate-capped PbS NCs and (B) 2-CP:PbS NCs following excitation at 804 nm. Blue contours denote absorption losses (photobleaching) whereas red/yellow contours signal induced absorptions. Note, in panel A, data for wavelengths below 780 nm has been multiplied by 2.5× for ease of comparison. Data measured near 804 nm is omitted due to noise associated with the white light continuum probe.

decorated with amine ligands and a single 2-CP molecule. For a detailed description of these calculations, see Section SVIII of the Supporting Information.

# ■ EXPERIMENTAL RESULTS

Absorption spectra of 2-CP, PbS NCs, and the combined 2-CP:PbS system are shown in Figure 1. Examining 2-CP's spectrum first (Figure 1, green), we find it consists of a primary peak at 651 nm associated with its  $S_0 \rightarrow S_1$  transition. This peak is followed by a Franck–Condon progression with an energy spacing of ~1360 cm<sup>-1</sup> attributed to C–C stretching of the central pentacene group. The energies and relative oscillator strengths of 2-CP's electronic resonances are nearly identical to unfunctionalized TIPS-pentacene. <sup>36,37</sup> This suggests the

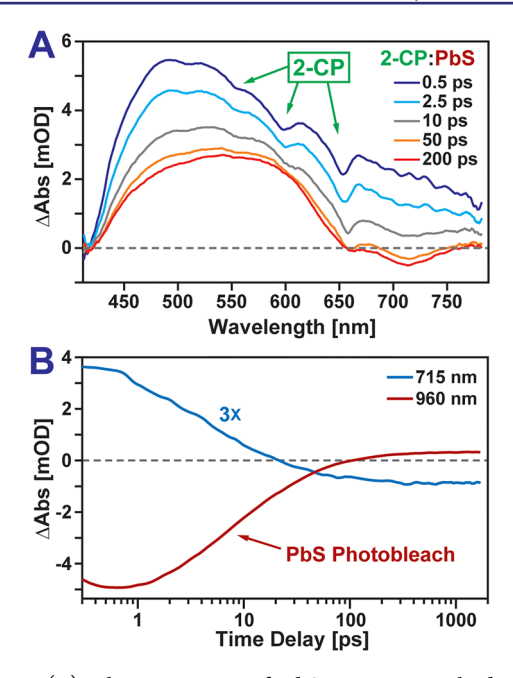


**Figure 3.** (A) Photoexcitation of PbS at 804 nm leads to the immediate appearance of 2-CP bleaching features that decay over  $\sim$ 40 ps. (B) 2-CP:PbS TA kinetics measured at different probe wavelengths highlight that as the PbS X1 bleach decays ( $\lambda_{\text{probe}} = 960$  nm; red) a new species appears that gives rise to a photobleach ( $\lambda_{\text{probe}} = 715$  nm; blue).

addition of a phenyl-based linker at the 2 position of 2-CP's pentacene core has a negligible impact on the character of the ground and lowest energy singlet exciton. Consequently, we take the character of the corresponding lowest triplet exciton to be similarly unperturbed. Though different energies for TIPS-pentacene triplet excitons have been reported, <sup>20,38</sup> a reasonable upper bound is 0.86 eV, <sup>36,39</sup> the value reported for unsubstituted pentacene. <sup>40–43</sup> As such, we estimate the energy of 2-CP triplet excitons to be no greater than 0.86 eV. Given the singlet exciton energy of 2-CP is 1.90 eV, formation of this state from pairs of 2-CP triplet excitons would require significant thermal activation. Thus, if exciton transfer from PbS NCs to 2-CP proves efficient, we expect 2-CP triplet excitons to be the dominant end species formed by PbS NC photoexcitation.

We use a ligand exchange process (see methods) to covalently attach 2-CP to PbS NCs that possess a lowestenergy exciton resonance peaked at 1005 nm. In keeping with prior work on semiconductor NCs, we denote the lowest energy exciton of our PbS NCs as their X1 state. 44-47 On the basis of the rising edge of the NC absorption spectrum, we estimate the lower bound on the energy of the NCs' X1 state to be ~1.1 eV, indicating excitons created by NC photoexcitation should have sufficient energy to produce a 2-CP triplet exciton. Following ligand exchange, we find the absorption spectrum of 2-CP-functionalized PbS NCs (2-CP:PbS) largely resembles a linear combination of the individual absorption profiles of 2-CP and PbS NCs, suggesting electronic coupling between these materials is weak. However, subtraction of the NC contribution to the absorption spectrum of 2-CP:PbS (Figure 1, inset) reveals the absorption resonances associated with 2-CP's  $S_0 \rightarrow S_1$ transition are shifted to lower energy by 13 meV upon binding to 2-CP. As the relative amplitude of peaks forming the Franck—Condon progression display only minor changes upon

PbS attachment, we assign this to a solvatochromic shift of 2-CP's  $S_0 \rightarrow S_1$  transition due to a change in 2-CP's dielectric environment when placed next to PbS. Comparison of the relative amplitude of the 2-CP and X1 absorption bands to extinction spectra measured for 2-CP ( $\varepsilon=19~200~{\rm M}^{-1}~{\rm cm}^{-1}$  at  $\lambda_{\rm max}=651~{\rm nm}$ ) and reported for PbS NCs³³ indicate 25.7 2-CP molecules are present in solution for each PbS NC. As excess 2-CP in solution has been removed by redispersing 2-CP functionalized PbS NCs in toluene, a solvent where 2-CP has negligible solubility, the majority of 2-CP molecules in solution are likely associated with the PbS NCs.

To assess the ability of PbS NCs to donate triplet excitons to 2-CP, we used transient absorption (TA) to track the dynamics of photoexcited excitons in PbS NCs. Figure 2A displays a contour map illustrating TA spectra measured for oleate-capped PbS NCs following excitation at 804 nm. Immediately upon excitation, a prominent negative feature appears at 990 nm that corresponds to a decrease of absorption (photobleach) of the NC's X1 band. As the electronic structure of PbS yields an identical number of valence and conduction band states contributing to the NCs' X1 transition, the presence of an electron in the lowest energy state of the conduction band or a hole in the highest energy state of the valence band will equally contribute to the photobleaching signal.<sup>48-52</sup> We note the spectral maximum of the X1 photobleach is shifted to higher energy relative to the peak of the X1 band's ground state absorption spectrum due to interference with an induced absorption transition that appears on the low-energy side of the X1 band. This induced absorption feature is associated with the creation of a biexciton, which requires lower energy than the formation of single exciton due to Coulombic screening provided by the initially excited electron and hole. 53-55 At shorter wavelengths, positive induced absorption features appear that correspond to interband transitions of the photoexcited NC. 48,56,57 Over the range of time delays shown, ~2 ns, TA spectra remain largely static. Measurements performed over nanosecond-to-microsecond delays (Supporting Information, Figure S4) indicate photobleaching of the PbS bandedge exciton decays with a 2  $\mu s$  time scale, consistent with prior reports of exciton lifetimes. 11,58-62

Following functionalization with 2-CP, TA spectra of PbS NCs display drastically different kinetics (Figure 2B). Similar to oleate-capped NCs, following NC photoexcitation we observe a loss of absorption near 960 nm arising from excitation of the NCs' X1 state. However, unlike oleate-capped NCs, we find this feature decays rapidly, and is completely quenched within the first 100 ps following excitation. To determine if this rapid decay of the NC X1 state arises from triplet energy transfer to 2-CP, we shift our focus to the visible spectral range. 2-CP triplet excitons should give rise to two spectral features in a TA measurement: (1) a negative photobleach mirroring 2-CP's ground state absorption due to depletion of its ground state, and (2) positive triplet induced absorption bands, which are expected to appear near 525 nm based on prior work on TIPSpentacene and related derivatives. 20,36,63-66 If PbS NCs transfer triplet excitons to 2-CP, these features will rise as the NC X1 photobleach decays.

However, in the visible range we see evolution of spectral features that differs from this expectation. Rather than growing in as the NC X1 band decays, sharp dips in the TA spectra can be seen at 554, 598, and 653 nm immediately upon photoexcitation whose positions agree well with the vibronic progression featured in 2-CP's ground state absorption

spectrum (Figure 3A). Interestingly, as the pump—probe time delay increases, we find these bands decay on a time scale identical to the NC X1 photobleach. This behavior is unexpected assuming their appearance is due to triplet energy transfer from PbS to 2-CP. Rather, the concerted dynamics of these transient spectral features and the photobleach of PbS's X1 resonance suggest bleaching of 2-CP's absorption transitions is induced by the presence of the X1 exciton.

Similar prompt photobleaching of acene ligands attached to PbS NCs has been observed by Garakyaraghi et al.<sup>20</sup> and attributed to a transient change in the electric field projected onto attached 2-CP molecules due to the generation of charge carriers within the associated PbS NC. Such electrostatic changes can shift the energy gaps between the electronic states of surface-bound ligands via the Stark effect, 67-70 leading to the appearance of a photobleach resembling their ground state absorption profile. These bleaches decay as excited charge carriers are removed from NC bandedge states. Similar to Garakyaraghi et al., 20 we attribute the appearance of 2-CP photobleaching features upon PbS photoexcitation to Starkinduced shifting of 2-CP's  $S_0 \rightarrow S_1$  transition. Importantly, as we show below, the decay of these features provides us with information that allows us to identify key steps involved in the transfer of energy from PbS to 2-CP.

At longer time delays, we find an additional photobleach appears at 715 nm (Figure 3B) as the photobleach of the NCs' X1 band decays, indicating the formation of a new electronic species. The growth of this band is accompanied by a decrease in amplitude and narrowing of the induced absorption transitions associated with NC interband transitions seen near 525 nm. These spectral features differ from those expected for 2-CP triplet excitons as no discernible 2-CP photobleach can be seen, indicating the removal of charge carriers from PbS's valence and conduction band does not directly yield 2-CP triplet excitons. Figure 4A displays the evolution of TA spectra of 2-CP:PbS NCs over delays ranging from 5 to 200 ns. Over this time range, we find the bleach appearing at 715 nm decays to baseline with a time constant of 113 ns. Concomitant with this change, the broad induced absorption band centered near 550 nm narrows and increases in amplitude to yield a new band centered at 535 nm. New photobleaches centered at 607 and 657 nm also appear over this time scale. The placement of these bands suggests the intermediate state formed during the decay of NC excitons subsequently evolves over ~100 ns to yield 2-CP triplet excitons.

To verify this hypothesis, we use a spectral decomposition model<sup>71-73</sup> (Supporting Information, Section SII) to fit our TA spectra and isolate the spectral component that grows in over ~100 ns. Comparison of this line shape to the 2-CP triplet line shape produced via photosensitization by platinum octaethylporphyrin in dichloromethane yields a striking resemblance (Figure 4B). Though features that appear in the line shape extracted from 2-CP:PbS TA spectra are shifted to lower energy, this shift is comparable to that seen between absorption spectra of 2-CP dissolved in toluene and 2-CP bound to PbS NCs (Figure 1, inset). Thus, we conclude photoexcitation of PbS NCs produces 2-CP triplet excitons over 113 ns. This rate is consistent with other reports that have observed triplet energy transfer from semiconductor NCs to acenes over tens to hundreds of nanoseconds. 11,15,18-20 Over longer time scales, we find 2-CP triplets return to the ground state with a lifetime of 1.7  $\mu$ s. Thus, as surmised in the Jablonski plot in Scheme 1, 2-CP triplet excitons are the final excited state formed in the

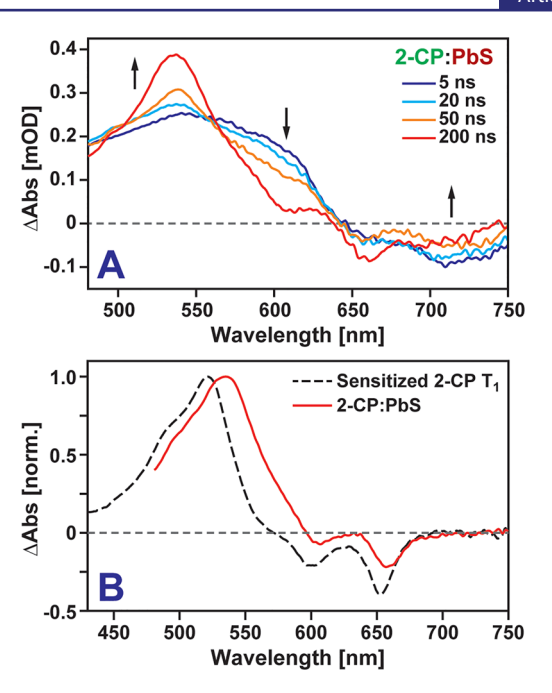


**Figure 4.** (A) TA spectra of 2-CP:PbS NCs following excitation at 1064 nm. (B) Transient spectrum of 2-CP triplet excitons determined from solution phase sensitization measurements (black dashed) and a spectral component extracted from TA spectra of 2-CP:PbS NCs that grows with a 113 ns time constant (red solid). The good agreement between these lineshapes suggests infrared excitation of 2-CP:PbS produces 2-CP triplet excitons over ~100 ns.

system. Interestingly, this relaxation rate is  $\sim$ 7× faster than the lifetime we determine for free 2-CP molecules in solution (11.6  $\mu$ s, Supporting Information, Figure S6), suggesting the adherence of 2-CP to PbS enhances the rate of triplet decay to the ground state. This observation is in alignment with reports from other groups that have found accelerated triplet lifetimes for acenes bound to NCs.  $^{21,22}$ 

# DISCUSSION

Our data demonstrate infrared excitation of PbS NCs results in 2-CP triplet exciton formation. However, the kinetics we measure indicate this process does not proceed directly from charge carriers in the valence or conduction bands of PbS. Rather, an intermediate state is formed from the PbS X1 state within ~40 ps leading to a broad photobleach at 715 nm and no discernible photobleaching features of the 2-CP ligand (Figure 3A, red trace). Spectral features from this intermediate decay as triplet excitons are created (Figure 4A). Prior work by Garakyaraghi et al. on PbS NCs functionalized with a TIPSpentacene ligand similarly found the rate of pentacene triplet exciton generation did not match the recovery rate of the PbS NC X1 photobleach following PbS photoexcitation.<sup>20</sup> On the basis of the close energy alignment of TIPS-pentacene's HOMO level and the valence band of PbS, the authors of this study suggested pentacene triplet excitons were produced by two sequential charge transfer events, with hole transfer from PbS to TIPS-pentacene occurring over tens of picoseconds followed by electron transfer on nanosecond time scales. However, this hypothesis is not fully supported by their data as the formation of TIPS-pentacene cations should induce a photobleach of the ligand absorption bands based on their spectroelectrochemical assignment, yet this feature is not observed on picosecond time scales. In addition, the presence

of an electron in the conduction band of PbS should give rise to a photobleach of the NC X1 band, but this feature fully recovers prior to the development of spectral features attributed to TIPS-pentacene triplet excitons. The spectral intermediate we identify lacks photobleaching from 2-CP and the NC X1 band, thus we similarly cannot assign its origin to hole transfer from PbS to 2-CP.

We have also considered the formation of TIPS-pentacene excimers as the physical basis for the spectral intermediate we observe. A prior study of concentrated TIPS-pentacene solutions found photoexciting aggregates formed in solution produces an excimer state that generates triplet exciton pairs via singlet fission.<sup>36</sup> Importantly, TIPS-pentacene excimers were identified in TA measurements through the appearance of a stimulated emission band centered at 715 nm that is not unlike the photobleaching transition we associate with our spectral intermediate. However, excimer formation in the system we investigate here would require the absorption of multiple photons by PbS as the energy of a TIPS-pentacene excimer is larger than that of the 804 nm photons used to excite our NCs. As such, excimer formation seems unlikely as TA spectra measured using excitation densities as low as 0.07 excitations/ NC display spectral dynamics identical to those in Figures 2–4 (Supporting Information, Figure S5). Moreover, we have verified that increasing the excitation density to produce multiple excitations per NC does not lead to an enhanced growth of the photobleaching feature at 715 nm. Rather up to an average excitation density of 3 excitations per NC, this band scales linearly with pump fluence (vide infra), suggesting it is produced upon absorption of a single photon. Thus, we rule out excimer formation as the origin of the 715 nm band as well.

One additional hypothesis that could explain the intermediate we observe is it represents localized charge carrier/exciton states formed at the surface of PbS NCs. Incomplete or poor passivation of atoms at PbS NC surfaces has previously been implicated in the formation of midgap states that alter their photoluminescent properties. The surface defects have also been implicated in the creation of trap states that hamper carrier migration in PbS NC solids. In some cases, the introduction of surface defects has been tied to the exchange of ligands bound to NC surfaces. As we illustrate below, both TA spectra and DFT calculations present a case for exciton migration to PbS surface sites prior to their transfer to 2-CP ligands.

To better examine the mechanism leading to the formation of the kinetic intermediate we identify, we have used a spectral decomposition model  $^{71-73}$  to analyze the evolution of our TA spectra on subnanosecond time scales. In brief, this model divides TA spectra into a linear combination of basis spectra whose amplitudes are governed by sequential first-order kinetic interconversions as a function of time (Supporting Information, Section SII). Figure 5A displays the three spectral components that contribute to TA spectra of 2-CP:PbS NCs over the first nanosecond following photoexcitation at 804 nm. Immediately upon excitation of PbS, we observe a bleaching of its X1 band due to the excitation of an electron from the NC's valence band to its conduction band. At shorter wavelengths, features associated with Stark-induced changes in 2-CP ligand absorption bands appear (Figure 5A, dark blue). Over time, both spectral features decay, concomitant with the development of a photobleach at 715 nm (Figure 5A, red). Interestingly, we find these time-dependent changes cannot be adequately described using a single first-order time constant. Rather, two

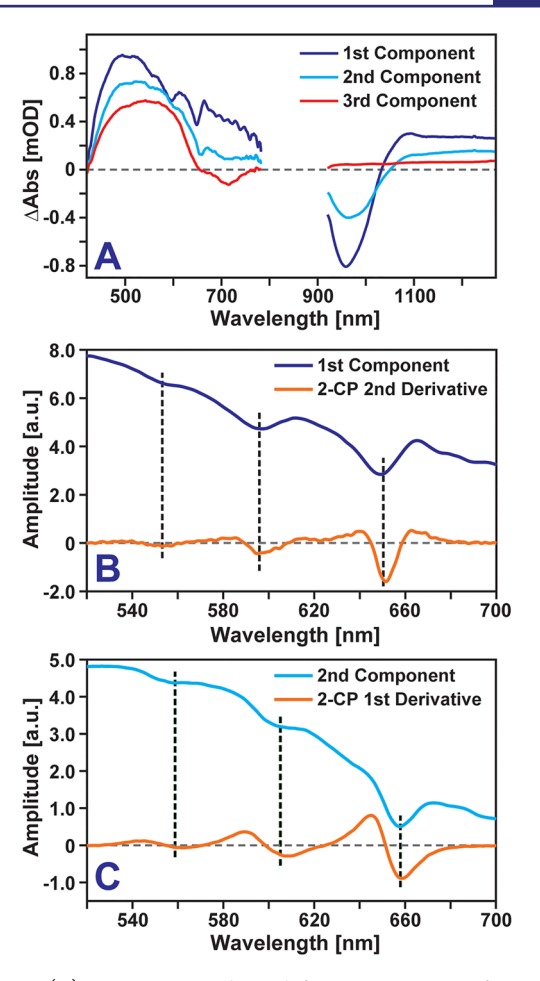


Figure 5. (A) Basis spectra derived from TA spectra of 2-CP:PbS NCs. TA spectra initially resemble the 1st component (dark blue) and evolve over a few picoseconds to resemble a spectrum described by the 2nd component (cyan). The spectra continue to evolve over tens of picoseconds to resemble the 3rd component (red). For ease of comparison, component amplitudes for wavelengths below 800 nm have been multiplied by 2.5. (B) Comparison of the 1st spectral component and the 2nd derivative of 2-CP's absorption spectrum. (C) Comparison of the 2nd spectral component and the 1st derivative of 2-CP's absorption spectrum. Dashed black lines in panels B and C are drawn to aid comparison of spectral features.

time constants, with values of 3.3 and 37 ps are required to adequately describe the TA spectral evolution.

To determine the origin of the faster event, we focus on the visible region of the first two spectral components extracted with our decomposition model. Examining the first component, which describes the line shape of the TA signal immediately upon photoexcitation (Figure 5B), we find it consists of a broad induced absorption associated with interband transitions of the excited PbS NC. Superimposed on this background are a series of narrow induced absorptions and bleaches due to Starkinduced shifting of 2-CP's ground state absorption line shape. Plotted above the first component is the second derivative of 2-CP's absorption line shape, which is composed of positive and negative features that agree well with the maxima and minima of Stark-shifted 2-CP bands appearing in the TA line shape. This agreement can be interpreted as a subset of 2-CP molecules experiencing a local electric field that shifts their absorption resonances to lower energy whereas others experience a field that pushes their resonances toward higher

energy. The direction an absorption resonance shifts is set by the sign of the field, suggesting the photoexcited electron and hole produce a dipolar field that causes some 2-CP ligands to experience a net negative field whereas others experience a net positive field. For additional details regarding this spectral assignment, we direct interested readers to Section SIII of the Supporting Information.

The TA line shape in Figure 5B evolves with a rate of 1/3.3 ps<sup>-1</sup> to the spectrum in Figure 5C. Similar to the line shape in Figure 5B, the spectrum in Figure 5C consists of a broad induced absorption stemming from carriers in PbS with superimposed induced absorptions and bleaches associated with 2-CP ligands. However, the 2-CP features in this line shape are distinct from those observed immediately upon photoexcitation and agree well with the first derivative of 2-CP's absorption spectrum rather than its second. The shift in position of 2-CP absorption features suggests changes observed in TA spectra over 3.3 ps correspond to a process that alters the electric field distribution felt by 2-CP ligands from a dipolar field to one of more uniformity that, on average, shifts the absorption resonances of bound ligands in the same spectral direction.

One explanation for this spectral evolution is localization of either the photoexcited electron or hole at the PbS NC's surface. In such a scenario, 2-CP ligands attached to the NC, spatially distant from the localized carrier, would feel a reduced field. The behavior of their absorption resonance would be subsequently dominated by the oppositely signed carrier remaining in the NC core. Averaging over the distribution of fields felt by attached 2-CP ligands in this case would result in most ligands experiencing a field with a uniform sign that shifts their absorption resonances in a singular direction. The amplitudes of the NC X1 bleach associated with the first and second components extracted from our spectral decomposition model provide additional support for this hypothesis. Figure 5A shows the X1 bleach experiences a ~50% amplitude reduction as our TA spectra evolve from the first component to the second. As both the photoexcited electron and hole contribute equally to the X1 photobleach, 48-52 removing one of these carriers from the NC core and placing it in a localized surface state would reduce the X1 photobleach by 50%. Thus, we assign the 1/3.3 ps<sup>-1</sup> rate we extract from our TA spectra to localization of either the excited electron or hole at the PbS NC surface.

With passing time, we observe a complete loss of bleaching features from both 2-CP and the NC X1 band as evidenced by the absence of these features in the third spectral component in Figure 5A. These changes, unfolding with a kinetic rate of 1/37 ps<sup>-1</sup>, suggest that upon singular carrier localization at the PbS NC surface, the second photoexcited carrier localizes as well. Interestingly, the presence of a long-lived X1 photobleach in our TA measurements of neat PbS NCs indicates localized surface states are not intrinsic to the oleate-capped PbS NCs we studied, but are rather induced by the ligand exchange process used to functionalize these NCs with 2-CP. We suspect the size disparity between 2-CP and oleate may hint at the potential mechanism that underlies the creation of sites for localized surface states. Because of its pendant TIPS groups, 2-CP is expected to occupy a larger area on PbS surfaces than oleate. As such, oleates near a binding site with an exchanged 2-CP ligand likely deform their structure to some degree to accommodate this larger ligand. Additionally, steric repulsion between these oleates and 2-CP could weaken oleate binding and enhance

their probability for desorbing from the NC surface. As oleate is charged, it may desorb not as an anion but as a  $Pb^{2+}(oleate)_2$  coordination complexe, <sup>83</sup> creating unpassivated  $S^{2-}$  sites that could localize photoexcited holes. If occurring in high enough yield, such ion loss would likely lead to etching of PbS that should be observable as a blue shift of their lowest exciton band. Indeed, when we treat oleate-capped PbS with a 500:1 excess of 2-CP ligands, we observe a slight blue-shift of their X1 band (Supporting Information, Figure S7), providing evidence in favor of this scenario.

Localized surface states could conceivably impact triplet energy transfer in a few different ways. The formation of a localized state near a 2-CP ligand may improve wave function overlap and facilitate triplet energy transfer. Alternatively, if localized states form at surface sites spatially distant from 2-CP ligands, such states can substantially hamper triplet transfer as excitations must either transfer back to the NC core or diffuse along the NC surface 84,85 to find a 2-CP molecule. To examine the nature of different states present in 2-CP:PbS NCs, we have used constrained DFT to investigate their electronic structure. The system we have examined consists of a 1.5 nm diameter PbS NC (76 Pb and 76 S atoms) arranged in a rock salt structure. A single 2-CP molecule is attached to the PbS surface and other surface sites are terminated with amine ligands. 15,86 The amine ligands were chosen for computational simplicity: the monodentate headgroup induces less surface rearrangement than a carboxylate, making it less necessary to perform timeconsuming geometric relaxation of the structure. 85,87 Though this system employs a small PbS NC core as well as L-type passivating ligands (amines) in place of the X-type ligands (carboxylates) used experimentally, we postulate the qualitative results obtained for this system are likely to hold for the 2-CP:PbS NCs we have explored using time-resolved measure-

As expected, by applying appropriate constraints to the 2-CP-NC model we identify spin-triplet states localized within the NC core and 2-CP moiety (Figure 6A). Surprisingly, however, we find that in addition to the delocalized, bulk-like exciton there are also multiple surface excitons on the NC, two of which are shown in Figure 6B,C. The existence of these surface states runs contrary to conventional wisdom about PbS NCs of this size. Because the NC diameter (1.5 nm) is far smaller than the bulk exciton radius (20 nm), the simplest picture would assert that all excitons are confined to particle-in-a-sphere-like states. 88,89 There would thus be only one low-lying, bulk-like exciton and all surface states would be much higher in energy. The existence of these surface states can however be rationalized on two fronts. First, the surface atoms are undercoordinated compared to the bulk, shifting their energies and favoring surface localization. 85,90,91 Second, the binding of 2-CP to a surface atom can affect its displacement with respect to the NC core, which can also act to produce localized surface states.

Though it is beyond the scope of this work to exhaustively characterize these surface triplet states, at a bare minimum we identify a state strongly associated with the PbS NC surface that is localized near the 2-CP ligand (Figure 6B). This state has energy comparable to that of a spin-triplet exciton in the NC core and is spatially much closer to the 2-CP ligand, which will facilitate the kind of wave function overlap required for triplet transfer. These aspects suggest surface states of this type may serve as an intermediate for triplet energy transfer to 2-CP. Importantly, however, we also identify additional spin-triplet states at the PbS surface that have negligible interaction with

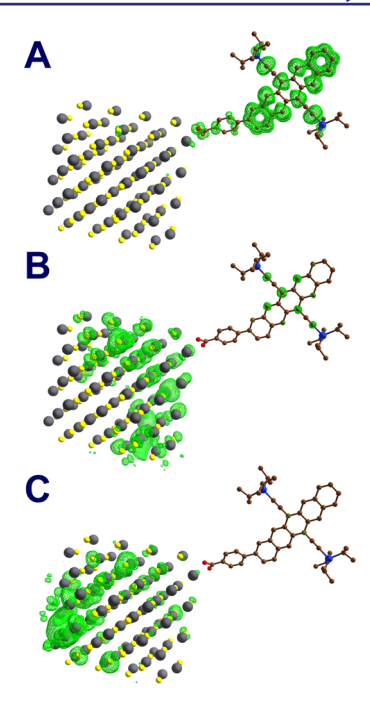


**Figure 6.** Illustration of different spin-triplet states identified via constrained DFT calculations that are associated with (A) the 2-CP ligand and (B and C) the PbS NC surface. In each panel, the green surfaces correspond to the spin density associated with the pictured spin-triplet state. Panel B highlights a surface state that is a potential transition state for triplet energy transfer to 2-CP whereas panel C displays a surface-localized state wherein a triplet exciton is spatially distant from the 2-CP molecule. Note, amine ligands bound to each NC surface are omitted to aid visualization of the spin density of electronically excited states pictured in panels A–C.

the 2-CP ligand. An example of such a state is shown in Figure 6C. Like the transition state we identify, we find this second localized state has an energy similar to that of a spin-triplet exciton delocalized throughout the PbS core, suggesting photoexcitation of PbS can also yield localized excitons that have negligible interaction with surface-bound 2-CP molecules. We hypothesize localized states of this type, which are weakly coupled to 2-CP molecules, are responsible for the slow NC-to-acene triplet transfer ( $\sim$ 100 ns) time scale we observe.

To vet our hypothesis that a subset of surface states hinders triplet transfer by localizing excitons in states weakly coupled to 2-CP molecules, we have examined how the rate of triplet production varies as the number of excitations simultaneously produced in a NC are increased. If a subset of surface states hinders triplet transfer, then producing sufficient excitations within a NC to saturate these sites should allow for more rapid triplet exciton production. Figure 7A plots how the amplitude of the TA signal measured for 2-CP:PbS NCs at a pump probe time delay of 1.75 ns varies as a function of pump fluence. This is a time delay at which charge carriers have localized at surface sites, but 2-CP exciton formation has yet to occur. We monitor the strength of the signal at 715 nm as we now understand this signal to arise from photobleaching of interband transitions that are modified by the population of surface-localized states. We find as the intensity of the pump pulse that excites the NCs is increased, the amplitude of the surface state signal increases linearly up to a point where ~3 excitations have been produced per NC. After this point, the signal plateaus, suggesting we have saturated surface-localized PbS states.

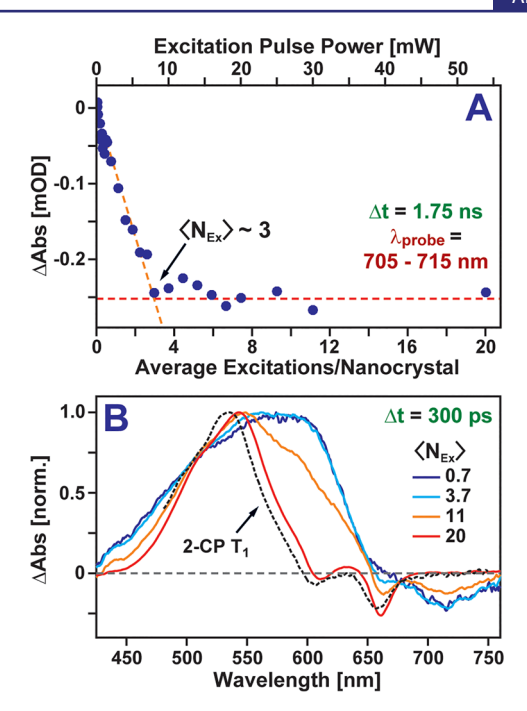


Figure 7. (A) 2-CP:PbS TA signal amplitude at a time delay of 1.75 ns integrated from 705 to 715 nm. Above an average excitation density of  $\sim$ 3 excitations per NC, the signal amplitude saturates. (B) 2-CP:PbS TA spectra measured at a time delay of 300 ps as a function of excitation density. As the average number of excitations per NC is increased above 3, features resembling 2-CP triplet excitons (black dashed) appear.

Figure 7B displays TA spectra measured at a delay of 300 ps, normalized to their maximum amplitude. Below an average excitation density of 3 excitations per NC, these spectra are nearly indistinguishable; indicating the number of surface states we populate grows linearly with excitation density. However, above this value, we find the line shape gradually transforms into one characteristic of 2-CP triplets. Fitting the triplet production kinetics, we find the time scale of this process increases from 113 ns to ~50 ps for average excitation densities above 3 excitations per NC, indicating saturating surface states significantly speeds triplet exciton transfer. Considering that the number of surface states we need to saturate is small compared to the number of ligands we bind to a NC, it is unlikely that carriers rapidly diffuse between states on a NC surface. Instead, we hypothesize carriers spend long residence times in a small number of surface trap states that hinder triplet transfer to 2-CP.

Though the increase in 2-CP triplet production rate suggests surface states slow transfer of triplet excitations to 2-CP until filled, given the high excitation densities we employ other explanations for our observations need to be considered. TA experiments performed on bare 2-CP molecules in solution show no signatures of two-photon absorption under the 804 excitation conditions we use for TA measurements described above. Two-photon absorption by PbS itself or Auger recombination of multiple excited carriers could generate high-energy NC excitations capable of radiatively producing 2-CP spin-singlet excitons. Such excitations may later convert to triplets via intersystem crossing or even singlet fission if the density of 2-CP ligands on the NC surface is sufficiently high to support this latter possibility. However, these scenarios require the formation of a 2-CP spin-singlet intermediate,

which is clearly absent from our TA spectra. Though subpicosecond singlet fission between 2-CP molecules could make the observation of a 2-CP singlet intermediate difficult to observe, the modest changes in 2-CP's absorption line shape upon binding of molecules to PbS suggest 2-CP molecules tethered to PbS surfaces only weakly interact with one another, which should suppress singlet fission.

Taken together, our results indicate the presence of surface-localized states on PbS NCs on average slow triplet energy transfer between the NC and bound acene ligands. On the basis of the inflection point of the fluence-dependent data in Figure 7A, we estimate that, on average, 3 localized sites exist per NC. Though our data does not, at present, allow us to discern if triplet excitons are produced directly from surface-localized states or from excitations that transfer back to the NC core and then to 2-CP, our fluence-dependent data suggests removing these states through improved passivation strategies may enhance triplet transfer rates. We are exploring this possibility.

# CONCLUSIONS

We have used ultrafast TA to examine energy transfer dynamics within a hybrid organic:inorganic system composed of PbS semiconductor NCs functionalized with 2-CP, a TIPSpentacene containing ligand. Excitation of PbS produces a spectroscopically identifiable intermediate over a 37 ps time scale that decays as 2-CP triplet excitons are created over ~100 ns. Analysis of TA lineshapes measured at early time delays indicates the intermediate results from states that localize excitations at the PbS NC surface. These states are not intrinsic to PbS NCs upon synthesis but are induced during 2-CP ligand exchange. Saturation of these surface states at high excitation densities speeds triplet exciton production, insinuating many of these states likely form at sites weakly coupled to 2-CP molecules and thereby slow triplet energy production. This scenario is supported by constrained DFT calculations that identify spin-triplet surface states that may serve as intermediates for energy transfer to 2-CP molecules and others that isolate excitons from 2-CP molecules. If these latter types of surface-localized sites can be eliminated via surface passivation strategies or ligand exchange methodologies, triplet energy transfer from PbS can likely be enhanced. Rather than acting as a passive bystander, our work highlights that the structure of NC surfaces can play an active role in mediating triplet energy transfer from NCs to surface-adhered ligands.

# ASSOCIATED CONTENT

## S Supporting Information

The Supporting Information is available free of charge on the ACS Publications website at DOI: 10.1021/jacs.8b01966.

Details regarding the synthesis of 2-CP; a description of the spectral model used to extract kinetic rates from transient absorption spectra; a discussion of Stark-induced spectral features in TA spectra; TA spectra of oleate-capped PbS NCs and 2-CP functionalized NCs for varying pump fluences; a description of sensitization experiments used to determine absorption features of 2-CP triplet excitons; evidence for etching of 2-CP nanocrystals during ligand exchange; and computational methodology employed for constrained density functional theory calculations (PDF)

#### AUTHOR INFORMATION

# Corresponding Author

\*roberts@cm.utexas.edu

## ORCID (

Jon A. Bender: 0000-0003-1713-1480

Pan Xia: 0000-0001-8615-3590

Ming Lee Tang: 0000-0002-7642-2598 Sean T. Roberts: 0000-0002-3322-3687

# **Author Contributions**

<sup>1</sup>These two authors contributed equally.

#### Notes

The authors declare no competing financial interest.

# ACKNOWLEDGMENTS

Work performed at the University of Texas at Austin was supported by the Robert A. Welch Foundation (Grant F-1885) and the National Science Foundation (CHE-1610412). M.L.T. acknowledges support by the Alfred P. Sloan foundation and the National Science Foundation (CHE-1351663). Computational work was supported by the Center for Excitonics, an Energy Frontier Research Center funded by the U.S. Department of Energy, Office of Science, Office of Basic Energy Sciences under Award Number DE-SC0001088. We also acknowledge Delia J. Milliron and Michael J. Rose for access to gloveboxes maintained by their groups, which were used for sample preparation and storage.

# REFERENCES

- (1) Smith, M. B.; Michl, J. Chem. Rev. 2010, 110 (11), 6891-6936.
- (2) Smith, M. B.; Michl, J. Annu. Rev. Phys. Chem. 2013, 64, 361-386.
- (3) Tabachnyk, M.; Ehrler, B.; Gélinas, S.; Böhm, M. L.; Walker, B. J.; Musselman, K. P.; Greenham, N. C.; Friend, R. H.; Rao, A. *Nat. Mater.* **2014**, *13* (11), 1033–1038.
- (4) Thompson, N. J.; Wilson, M. W. B.; Congreve, D. N.; Brown, P. R.; Scherer, J. M.; Bischof, T. S.; Wu, M.; Geva, N.; Welborn, M.; Voorhis, T. V.; Bulović, V.; Bawendi, M. G.; Baldo, M. A. *Nat. Mater.* **2014**, *13*, 1039–1043.
- (5) Hanna, M. C.; Nozik, A. J. J. Appl. Phys. 2006, 100, 74510.
- (6) Tayebjee, M. J. Y.; McCamey, D. R.; Schmidt, T. W. J. Phys. Chem. Lett. 2015, 6 (12), 2367–2378.
- (7) Yang, L.; Tabachnyk, M.; Bayliss, S. L.; Böhm, M. L.; Broch, K.; Greenham, N. C.; Friend, R. H.; Ehrler, B. *Nano Lett.* **2015**, *15* (1), 354–358.
- (8) Ehrler, B.; Musselman, K. P.; Böhm, M. L.; Friend, R. H.; Greenham, N. C. *Appl. Phys. Lett.* **2012**, *101* (15), 153507–153507.
- (9) Huang, Z.; Tang, M. L. J. Am. Chem. Soc. 2017, 139 (28), 9412–9418.
- (10) Mongin, C.; Garakyaraghi, S.; Razgoniaeva, N.; Zamkov, M.; Castellano, F. N. Science 2016, 351, 369–372.
- (11) Wu, M.; Congreve, D. N.; Wilson, M. W. B.; Jean, J.; Geva, N.; Welborn, M.; Van Voorhis, T.; Bulović, V.; Bawendi, M. G.; Baldo, M. A. *Nat. Photonics* **2016**, *10* (1), 31–34.
- (12) Okumura, K.; Mase, K.; Yanai, N.; Kimizuka, N. Chem. Eur. J. 2016, 22 (23), 7721-7726.
- (13) Turro, N. J. Modern Molecular Photochemistry; University Science Books: Sausalito, CA, 1991.
- (14) Olaya-Castro, A.; Scholes, G. D. Int. Rev. Phys. Chem. 2011, 30 (1), 49–77.
- (15) Nienhaus, L.; Wu, M.; Geva, N.; Shepherd, J. J.; Wilson, M. W. B.; Bulović, V.; Van Voorhis, T.; Baldo, M. A.; Bawendi, M. G. ACS Nano 2017, 11 (8), 7848–7857.
- (16) Huang, Z.; Li, X.; Mahboub, M.; Hanson, K. M.; Nichols, V. M.; Le, H.; Tang, M. L.; Bardeen, C. J. *Nano Lett.* **2015**, *15* (8), 5552–5557.
- (17) Dexter, D. L. J. Chem. Phys. 1953, 21 (5), 836-836.

I

- (18) Li, X.; Huang, Z.; Zavala, R.; Tang, M. L. J. Phys. Chem. Lett. **2016**, 7 (11), 1955–1959.
- (19) Piland, G. B.; Huang, Z.; Lee Tang, M.; Bardeen, C. J. J. Phys. Chem. C 2016, 120 (11), 5883-5889.
- (20) Garakyaraghi, S.; Mongin, C.; Granger, D. B.; Anthony, J. E.; Castellano, F. N. J. Phys. Chem. Lett. 2017, 8 (7), 1458-1463.
- (21) Huang, Z.; Xu, Z.; Mahboub, M.; Li, X.; Taylor, J. W.; Harman, W. H.; Lian, T.; Tang, M. L. Angew. Chem., Int. Ed. 2017, 56 (52),
- (22) Kroupa, D. M.; Arias, D. H.; Carroll, G. M.; Granger, D. B.; Blackburn, J. L.; Anthony, J. E.; Beard, M. C.; Johnson, J. C. Nano Lett. 2018, 18 (2), 865-873.
- (23) Xia, P.; Huang, Z.; Li, X.; Romero, J. J.; Vulley, V. I.; Pau, G. S. H.; Tang, M. L. Chem. Commun. 2017, 53 (7), 1241-1244.
- (24) Bawendi, M. G.; Carroll, P. J.; Wilson, W. L.; Brus, L. E. J. Chem. Phys. 1992, 96 (2), 946-954.
- (25) Hässelbarth, A.; Eychmüller, A.; Weller, H. Chem. Phys. Lett. 1993, 203 (2-3), 271-276.
- (26) Nagpal, P.; Klimov, V. I. Nat. Commun. 2011, 2, 486.
- (27) Voznyy, O.; Sargent, E. H. Phys. Rev. Lett. 2014, 112 (15), 157401.
- (28) Krause, M. M.; Kambhampati, P. Phys. Chem. Chem. Phys. 2015, 17 (29), 18882-18894.
- (29) Boles, M. A.; Ling, D.; Hyeon, T.; Talapin, D. V. Nat. Mater. 2016, 15 (2), 141–153.
- (30) Huang, Z.; Li, X.; Yip, B. D.; Rubalcava, J. M.; Bardeen, C. J.; Tang, M. L. Chem. Mater. 2015, 27 (21), 7503-7507.
- (31) Sanders, S. N.; Kumarasamy, E.; Pun, A. B.; Trinh, M. T.; Choi, B.; Xia, J.; Taffet, E. J.; Low, J. Z.; Miller, J. R.; Roy, X.; Zhu, X.-Y.; Steigerwald, M. L.; Sfeir, M. Y.; Campos, L. M. J. Am. Chem. Soc. 2015, 137 (28), 8965-8972.
- (32) Mahboub, M.; Maghsoudiganjeh, H.; Pham, A. M.; Huang, Z.; Tang, M. L. Adv. Funct. Mater. 2016, 26 (33), 6091-6097.
- (33) Cademartiri, L.; Montanari, E.; Calestani, G.; Migliori, A.; Guagliardi, A.; Ozin, G. A. J. Am. Chem. Soc. 2006, 128 (31), 10337-10346.
- (34) Park, S.; Baranov, D.; Ryu, J.; Jonas, D. International Conference on Ultrafast Phenomena; OSA Technical Digest 2016, UW4A.23.
- (35) Wu, Q.; Van Voorhis, T. J. Phys. Chem. A 2006, 110 (29), 9212-9218.
- (36) Walker, B. J.; Musser, A. J.; Beljonne, D.; Friend, R. H. Nat. Chem. 2013, 5 (12), 1019–1024.
- (37) Hwang, D. K.; Fuentes-Hernandez, C.; Berrigan, J. D.; Fang, Y.; Kim, J.; Potscavage, W. J.; Cheun, H.; Sandhage, K. H.; Kippelen, B. J. Mater. Chem. 2012, 22 (12), 5531-5537.
- (38) Zirzlmeier, J.; Lehnherr, D.; Coto, P. B.; Chernick, E. T.; Casillas, R.; Basel, B. S.; Thoss, M.; Tykwinski, R. R.; Guldi, D. M. Proc. Natl. Acad. Sci. U. S. A. 2015, 112 (17), 5325-5330.
- (39) Sharifzadeh, S.; Wong, C. Y.; Wu, H.; Cotts, B. L.; Kronik, L.; Ginsberg, N. S.; Neaton, J. B. Adv. Funct. Mater. 2015, 25 (13), 2038-
- (40) Thorsmølle, V. K.; Averitt, R. D.; Demsar, J.; Smith, D. L.; Tretiak, S.; Martin, R. L.; Chi, X.; Crone, B. K.; Ramirez, A. P.; Taylor, A. J. Phys. Rev. Lett. 2009, 102, 17401-17401.
- (41) Chan, W.-L.; Ligges, M.; Jailaubekov, A.; Kaake, L.; Miaja-Avila, L.; Zhu, X.-Y. Science 2011, 334 (6062), 1541-1545.
- (42) Vilar, M. R.; Heyman, M.; Schott, M. Chem. Phys. Lett. 1983, 94 (5), 522-526.
- (43) Burgos, J.; Pope, M.; Swenberg, C. E.; Alfano, R. R. Phys. Status Solidi B 1977, 83 (1), 249-256.
- (44) Kambhampati, P. Acc. Chem. Res. 2011, 44 (1), 1–13.
- (45) Schnitzenbaumer, K. J.; Labrador, T.; Dukovic, G. J. Phys. Chem. C 2015, 119 (23), 13314–13324.
- (46) Azzaro, M. S.; Babin, M. C.; Stauffer, S. K.; Henkelman, G.; Roberts, S. T. J. Phys. Chem. C 2016, 120 (49), 28224-28234.
- (47) Turner, D. B.; Hassan, Y.; Scholes, G. D. Nano Lett. 2012, 12 (2), 880-886.
- (48) Klimov, V. I. Annu. Rev. Phys. Chem. 2007, 58, 635-673.
- (49) Schaller, R. D.; Klimov, V. I. Phys. Rev. Lett. 2004, 92, 186601.

- (50) Trinh, M. T.; Houtepen, A. J.; Schins, J. M.; Piris, J.; Siebbeles, L. D. A. Nano Lett. 2008, 8 (7), 2112-2117.
- (51) Gao, Y.; Talgorn, E.; Aerts, M.; Trinh, M. T.; Schins, J. M.; Houtepen, A. J.; Siebbeles, L. D. A. Nano Lett. 2011, 11 (12), 5471-
- (52) Gilmore, R. H.; Lee, E. M. Y.; Weidman, M. C.; Willard, A. P.; Tisdale, W. A. Nano Lett. 2017, 17 (2), 893-901.
- (53) Klimov, V. I. J. Phys. Chem. B 2000, 104 (26), 6112-6123.
- (54) Zhang, J.; Jiang, X. Appl. Phys. Lett. 2008, 92 (14), 141108.
- (55) Choi, Y.; Sim, S.; Lim, S. C.; Lee, Y. H.; Choi, H. Sci. Rep. 2013, 3 (1), 3206.
- (56) Yang, Y.; Rodríguez-Córdoba, W.; Lian, T. J. Am. Chem. Soc. 2011, 133 (24), 9246-9249.
- (57) Cho, B.; Peters, W. K.; Hill, R. J.; Courtney, T. L.; Jonas, D. M. Nano Lett. 2010, 10 (7), 2498-2505.
- (58) Knowles, K. E.; Malicki, M.; Weiss, E. A. J. Am. Chem. Soc. 2012, 134 (30), 12470-12473.
- (59) Clark, S. W.; Harbold, J. M.; Wise, F. W. J. Phys. Chem. C 2007, 111 (20), 7302-7305.
- (60) Gaponenko, M. S.; Lutich, A. A.; Tolstik, N. A.; Onushchenko, A. A.; Malyarevich, A. M.; Petrov, E. P.; Yumashev, K. V. Phys. Rev. B: Condens. Matter Mater. Phys. 2010, 82 (12), 125320.
- (61) Warner, J. H.; Thomsen, E.; Watt, A. R.; Heckenberg, N. R.; Rubinsztein-Dunlop, H. Nanotechnology 2005, 16 (2), 175-179.
- (62) Chen, Y.; Yu, D.; Li, B.; Chen, X.; Dong, Y.; Zhang, M. Appl. Phys. B: Lasers Opt. 2009, 95 (1), 173-177.
- (63) Pensack, R. D.; Tilley, A. J.; Parkin, S. R.; Lee, T. S.; Payne, M. M.; Gao, D.; Jahnke, A. A.; Oblinsky, D. G.; Li, P.-F.; Anthony, J. E.; Seferos, D. S.; Scholes, G. D. J. Am. Chem. Soc. 2015, 137 (21), 6790-
- (64) Grieco, C.; Doucette, G. S.; Pensack, R. D.; Payne, M. M.; Rimshaw, A.; Scholes, G. D.; Anthony, J. E.; Asbury, J. B. J. Am. Chem. Soc. 2016, 138 (49), 16069-16080.
- (65) Wu, Y.; Liu, K.; Liu, H.; Zhang, Y.; Zhang, H.; Yao, J.; Fu, H. J. Phys. Chem. Lett. 2014, 5, 3451-3455.
- (66) Musser, A. J.; Liebel, M.; Schnedermann, C.; Wende, T.; Kehoe, T. B.; Rao, A.; Kukura, P. Nat. Phys. 2015, 11 (4), 352-357.
- (67) Bublitz, G. U.; Boxer, S. G. Annu. Rev. Phys. Chem. 1997, 48, 2.13 - 2.42
- (68) Gélinas, S.; Rao, A.; Kumar, A.; Smith, S. L.; Chin, A. W.; Clark, J.; van der Poll, T. S.; Bazan, G. C.; Friend, R. H. Science 2014, 343,
- (69) Sebastian, L.; Weiser, G.; Bassler, H. Chem. Phys. 1981, 61, 125 - 135.
- (70) Ardo, S.; Sun, Y.; Castellano, F. N.; Meyer, G. J. J. Phys. Chem. B 2010, 114 (45), 14596-14604.
- (71) Vengris, M.; van der Horst, M. A.; Zgrablic, G.; van Stokkum, I. H. M.; Haacke, S.; Chergui, M.; Hellingwerf, K. J.; van Grondelle, R.; Larsen, D. S. Biophys. J. 2004, 87, 1848-1857.
- (72) Chen, X.; Larsen, D. S.; Bradforth, S. E.; van Stokkum, I. H. M. J. Phys. Chem. A 2011, 115 (16), 3807-3819.
- (73) Roberts, S. T.; Schlenker, C. W.; Barlier, V.; McAnally, R. E.; Zhang, Y.; Mastron, J. N.; Thompson, M. E.; Bradforth, S. E. J. Phys. Chem. Lett. 2011, 2, 48-54.
- (74) Peterson, J. J.; Krauss, T. D. Phys. Chem. Chem. Phys. 2006, 8 (33), 3851.
- (75) Gao, J.; Johnson, J. C. ACS Nano 2012, 6 (4), 3292-3303.
- (76) Fernée, M. J.; Thomsen, E.; Jensen, P.; Rubinsztein-Dunlop, H. Nanotechnology 2006, 17 (4), 956-962.
- (77) Caram, J. R.; Bertram, S. N.; Utzat, H.; Hess, W. R.; Carr, J. A.; Bischof, T. S.; Beyler, A. P.; Wilson, M. W. B.; Bawendi, M. G. Nano Lett. 2016, 16 (10), 6070-6077.
- (78) Park, B.; Whitham, K.; Bian, K.; Lim, Y.-F.; Hanrath, T. Phys. Chem. Chem. Phys. 2014, 16 (47), 25729-25733.
- (79) Zhitomirsky, D.; Voznyy, O.; Levina, L.; Hoogland, S.; Kemp, K. W.; Ip, A. H.; Thon, S. M.; Sargent, E. H. Nat. Commun. 2014, 5, 3803.
- (80) Cao, Y.; Stavrinadis, A.; Lasanta, T.; So, D.; Konstantatos, G. Nat. Energy 2016, 1 (4), 16035.

- (81) Hughes, B. K.; Ruddy, D. A.; Blackburn, J. L.; Smith, D. K.; Bergren, M. R.; Nozik, A. J.; Johnson, J. C.; Beard, M. C. *ACS Nano* **2012**, *6* (6), 5498–5506.
- (82) Zhitomirsky, D.; Voznyy, O.; Hoogland, S.; Sargent, E. H. ACS Nano 2013, 7 (6), 5282–5290.
- (83) Anderson, N. C.; Hendricks, M. P.; Choi, J. J.; Owen, J. S. J. Am. Chem. Soc. **2013**, 135 (49), 18536–18548.
- (84) Utterback, J. K.; Grennell, A. N.; Wilker, M. B.; Pearce, O. M.; Eaves, J. D.; Dukovic, G. *Nat. Chem.* **2016**, 8 (11), 1061–1066.
- (85) Voznyy, O. J. Phys. Chem. C 2011, 115 (32), 15927-15932.
- (86) Geva, N.; Shepherd, J. J.; Nienhaus, L.; Bawendi, M. G.; Van Voorhis, T. Morphology of Passivating Organic Ligands around a Nanocrystal. *ArXiv Prepr. ArXiv170600844*, 2017.
- (87) Kilina, S.; Velizhanin, K. A.; Ivanov, S.; Prezhdo, O. V.; Tretiak, S. ACS Nano **2012**, 6 (7), 6515–6524.
- (88) Wise, F. W. Acc. Chem. Res. 2000, 33 (11), 773-780.
- (89) Efros, A. L.; Efros, A. L. Sov Phys. Semicond 1982, 16 (7), 772-775.
- (90) Voznyy, O.; Thon, S. M.; Ip, A. H.; Sargent, E. H. J. Phys. Chem. Lett. 2013, 4 (6), 987-992.
- (91) Ip, A. H.; Thon, S. M.; Hoogland, S.; Voznyy, O.; Zhitomirsky, D.; Debnath, R.; Levina, L.; Rollny, L. R.; Carey, G. H.; Fischer, A.; Kemp, K. W.; Kramer, I. J.; Ning, Z.; Labelle, A. J.; Chou, K. W.; Amassian, A.; Sargent, E. H. Nat. Nanotechnol. 2012, 7 (9), 577–582. (92) You, Z.-Q.; Hsu, C.-P. Int. J. Quantum Chem. 2014, 114 (2), 102–115.